Disorder−Order Transition in Mesoscopic Silica Thin Films

Nan Yao,[‡,§] Anthony Y. Ku,[†,‡,§] Nobuyoshi Nakagawa,[†,‡] Tu Lee,[†,‡] Dudley A. Saville,[†,‡] and Ilhan A. Aksay*[,†,‡]

Department of Chemical Engineering and Princeton Materials Institute, Princeton University, Princeton, New Jersey 08540

Received January 18, 2000

Electron microscopy has been used to study the mesoscopic (nanometer-level) and microscopic (micrometer-level) structural evolution of mesoscopic silica thin films grown at the air−water interface under dilute, acidic (pH < 2) conditions. Transmission electron microscope observations reveal that the film begins with a disordered (amorphous) structure. Over time, mesoscopically ordered regions (hexagonally packed cylindrical channels) nucleate and grow within the film. Scanning electron microscopy reveals microscopic structural features such as ribbons, protrusions, domain boundaries, microindentations, and pits. Our work shows that mesoscopic order develops within the film through a "disorder to order transition." Our observations also clarify the role of the air−water interface in confining film growth to two dimensions during the initial stages. We note that a two-dimensional (in-plane) to three-dimensional (unconstrained) growth transition occurs when the film exceeds a critical thickness. We extend the current understanding of the structural evolution of the film by providing a detailed mechanism for the development of mesoscopic order and microscopic features and consider the possibility of a universal growth mechanism for films and particles.

Introduction

There is much interest in tailoring the structure of mesoscopic silica effected by the organization of organic structure-directing agents (i.e., surfactants, block copolymers).[1−33] The ultimate commercial success of this material depends on the ability to simultaneously control the morphology at multiple length scales (that is, from the nanometer-sized channels, to the packed channel domains, to the bulk structure). To date, particles,[2−15]

* To whom correspondence should be addressed. Phone: (609) 258-4393. Fax: (609) 258-6835 or 0211. E-mail: iaksay@princeton.edu

† Department of Chemical Engineering.

‡ Princeton Materials Institute.

§ These authors contributed equally to this work.

(1) Yanagisawa, T.; Shimizu, T.; Kuroda, K.; Kato, C. *Bull. Chem. Soc. Jpn.* **1997**, *63*, 988.

(2) Kresge, C. T.; Leonowicz, M. E.; Roth, W. J.; Vartuli, J. C.; Beck, J. S. *Nature* **1992**, *359*, 710.

(3) Vartuli, J. C.; Schmitt, K. D.; Kresge, C. T.; Roth, W. J.; Leonowicz, M. E.; McCullen, S. B.; Hellring, S. D.; Beck, J. S.; Schlenker, J. L.; Olson, D. H.; Sheppard, E. W. *Chem. Mater.* **1994**, *6*, 2317.

(4) Huo, Q.; Margolese, D. I.; Ciesla, U.; Feng, P.; Gier, T. E.; Sieger, P.; Leon, R.; Petroff, P. M.; Schuth, F.; Stucky, G. D. *Nature* **1994**, *368*, 317.

(5) Huo, Q.; Margolese, D. I.; Ciesla, U.; Demuth, D. G.; Feng, P.; Gier, T. E.; Sieger, P.; Firouzi, A.; Chmelka, B. F.; Schuth, F.; Stucky, G. D. *Chem. Mater.* **1994**, *6*, 1176.

(6) Huo, Q.; Margolese, D. I.; Stucky, G. D. *Chem. Mater.* **1196**, *8*, 1147.

(7) Schacht, S.; Huo, Q.; Voigt-Martin, I. G.; Stucky, G. D.; Schuth, F. *Science* **1996**, *273*, 768.

(8) Zhao, D.; Feng, J.; Huo, Q.; Melosh, N.; Fredrickson, G. H.; Chmelka, B. F.; Stucky, G. D. *Science* **1998**, *279*, 548.

(9) Yang, H.; Ozin, G. A.; Kresge, C. T. *Adv. Mater.* **1998**, *10*, 883.

(10) Yang, H.; Coombs, N.; Ozin, G. A. *Nature* **1997**, *386*, 692.

(11) Yang, H.; Vovk, G.; Coombs, N.; Sokolov, I.; Ozin, G. A. *J. Mater. Chem.* **1998**, *8*, 743.

(12) Yang, H.; Coombs N.; Sokolov I.; Kresge C. T.; Ozin G. A. *Adv. Mater.* **1999**, *11*, 52.

(13) Schmidt-Winkel, P.; Yang, P.; Margolese, D. I.; Chmelka, B. F.; Stucky, G. D. *Adv. Mater.* **1999**, *11*, 303.

(14) McGrath, K. M.; Dabbs, D. M.; Yao, N.; Aksay, I. A.; Gruner, S. M. *Science* **1997**, *277*, 552.

(15) Lu, Y.; Fan, H.; Stump, A.; Ward, T. L.; Rieker, T.; Brinker, C. J. *Nature* **1999**, *398*, 223.

(16) Yang, H.; Coombs, N.; Sokolov, I.; Ozin, G. A. *Nature* **1996**, *381*, 589.

(17) Yang, H.; Coombs, N.; Dag, O.; Sokolov, I.; Ozin, G. A. *J. Mater. Chem.* **1997**, *7*, 1755.

(18) Aksay, I. A.; Trau, M.; Manne, S.; Honma, I.; Yao, N.; Zhou, L.; Fenter, P.; Eisenberger, P. M.; Gruner, S. M. *Science* **1996**, *273*, 892.

(19) Trau, M.; Yao, N.; Kim, E.; Xia, Y.; Whitesides, G. M.; Aksay, I. A. *Nature* **1997**, *390*, 674.

(20) Yang, H.; Coombs, N.; Ozin, G. A. *Adv. Mater.* **1997**, *9*, 811.

(21) Yang, P.; Deng, T.; Zhao, D.; Feng, P.; Pine, D.; Chmelka, B. F.; Whitesides, G. M.; Stucky, G. D. *Science* **1998**, *282*, 2244.

(22) Brown, A. S.; Holt, S. A.; Dam, T.; Trau, M.; White, J. W. *Langmuir* **1997**, *13*, 6363.

(23) Lu, Y.; Ganguli, R.; Drewien, C. A.; Anderson, M. T.; Brinker, C. J.; Gong, W.; Guo, Y.; Soyez, H.; Dunn, B.; Huang, M. H.; Zink, J. I. *Nature* **1997**, *389*, 364.

(24) Yang, H.; Kuperman, A.; Coombs, N.; Mamiche-Afara, S.; Ozin, G. A. *Nature* **1996**, *379*, 703.

(25) Yang, H.; Coombs, N.; Sokolov, I.; Ozin, G. A. *J. Mater. Chem.* **1997**, *7*, 1285.

(26) Yang, H.; Coombs, N.; Ozin, G. A. *J. Mater. Chem.* **1998**, *8*, 1205.

(27) To our knowledge, there is only one reported instance of successful film growth under alkaline conditions. See: Roser, S. J.; Patle, H. M.; Lovell, M. R.; Muir, J. E.; Mann, S. *Chem. Commun.* **1998**, *7*, 829.

(28) Brown, A. S.; Holt S. A.; Reynolds, P. A.; Penfold J.; White J. W. *Langmuir* **1998**, *14*, 5532.

(29) Holt, S. A.; Foran, G. J.; White, J. W. *Langmuir* **1999**, *15*, 2540.

(30) Ruggles, J. L.; Holt, S. A.; Reynolds, P. A.; Brown, A. S.; Creagh, D. C.; White, J. W. *Phys. Chem. Chem. Phys.* **1999**, *1*, 323.

(31) Feng, J.; Huo, Q.; Petroff, P. M.; Stucky, G. D. *Appl. Phys. Lett.* **1997**, *71*, 1887.

(32) Firouzi, A.; Atef, F.; Oertli, A. G.; Stucky, G. D.; Chmelka, B. F. *J. Am. Chem. Soc.* **1997**, *119*, 3596.

(33) Regev, O. *Langmuir* **1996**, *12*, 4940.

10.1021/cm000038a CCC: $19.00
Published on Web 06/19/2000

fibers,[7,9,13] and thin films[16−27] have been produced with varying pore sizes (5−30 nm)[2,3] and channel organization (i.e., hexagonal, cubic, and disordered bicontinuous, L_3).[2−4,7,16] It has also been shown that it is possible to influence the structure of mesoscopic materials at larger length scales.[2,15,18−21] While useful for predicting mesoscopic order, the earlier coassembly model[4,5] does not explain the physical mechanism by which mesoscopic (global/long-range) and microscopic order develop simultaneously from molecular level (local/surfactant−silicate) interactions. Although recent work has identified some important features as discussed below,[22,28−30] no comprehensive mechanistic description of the structural evolution exists. A more complete understanding of the mechanism, in particular during the early stages of mesophase formation, could lead to new and more effective ways of controlling the mesoscopic (pore structure and organization) and the microscopic features (morphology).

Although the first mesoporous materials were reported by Yanagisawa et al. in 1990,[1] they were not popularized until several years later when scientists at Mobil Research described a synthesis using subcritical, hydrothermal, alkaline processing conditions.[2,3] Shortly thereafter, workers at the University of California at Santa Barbara (UCSB group) showed that mesoscopic silica particles could be prepared under acidic conditions.[4,5] They reported that under acidic conditions the synthesis could be performed at lower temperatures while requiring less time and surfactant. It was also noted that, under these conditions, different microscopic morphologies may result. Mesoscopic silica thin films have been grown on solid substrates (e.g., graphite, mica, and silica) and at the air−water interface under acidic conditions.[9,16−18,23−26] Studies of thin films complement work done with particles and have led to an improved understanding of the mechanism.[7,11,17,18]

Although the exact mechanism of film growth is not well understood (as discussed below), it appears to involve deposition of silicate and surfactant precursors from solution at an interface. Manne and Gaub[34] used electrical double-layer atomic force microscopy (EDL-AFM) to image adsorbed surfactant layers on mica and graphite. They found that micelles adopt a cylindrical or hemicylindrical configuration depending on the substrate. Spheres and hemispheres were observed using different conditions.[35] Aksay et al.[18] demonstrated that this micellar organization at the interface is largely unchanged by the presence of silicate precursors. They also noted that interfacial interactions affect the micellar organization in two ways: (i) on most surfaces, the micellar structures are aligned parallel to the plane of the interface ("in-plane confinement"), and (ii) for strongly interacting substrates (e.g., graphite and mica), the micellar structures in each layer are further oriented along one or more preferred directions ("in-plane orientation").

Since the micelle diameters are much larger than the underlying lattice unit cell dimension, it is unlikely there is a direct lattice epitaxy effect. Rather, the interface may impose physical and/or energetic constraints on the first micellar layer, effectively confining it to the plane of the interface. Subsequent layers would be influenced by the configuration of the first layer. Two types of interfacial interactions may be responsible for in-plane confinement: (i) Helfrich-type bending energetic effects,[36] and/or (ii) electrostatic or other surface−micelle interactions. The Helfrich bending energy model predicts that micellar structures possess a spontaneous curvature in three dimensions. The presence of a surface restricts micellar motion, thereby creating an energetic incentive for in-plane confinement of the structure. Electrostatic and other energetic interactions may complement the Helfrich bending energy effect as well as cause in-plane orientation. The study of micellar organization at the air−water interface is difficult; no direct measurements of the morphology (using AFM or other techniques) are available. However, it may be possible to extrapolate the insights obtained from interfacial interactions with solid substrates to the more pliable air−water interface by treating it as a weakly interacting, hydrophobic surface.

In this study, we investigate the structural evolution of mesoscopic silica by focusing on films grown at the air−water interface in dilute, acidic (pH < 2) systems. This system offers several advantages. Films can be easily grown, collected, and characterized. Furthermore, there is a significant body of literature concerning both the final structure and temporal evolution. Finally, the air−water interface is an intermediate energetic environment between strongly interacting solid substrates and bulk solution (in the limit of no surface interaction, particles are formed).

Workers at the University of Toronto (Toronto group) have systematically examined mesoporous thin films grown under these conditions.[9,17,26] Powder and small-angle X-ray and neutron scattering (PXRD and SAXS, and SANS),[9,17,26] high-resolution scanning and transmission electron microscopy (HR−SEM and HR−TEM),[9,17,26] polarizing optical microscopy (POM),[17] laser confocal microscopy (LCM),[26] and AFM[9,17] have been employed. They also examined films grown on mica,[24] graphite,[25] and alkanethiol-coated gold.[20] Particles were studied using ^{29}Si nuclear magnetic resonance (^{29}Si NMR)[11] and dynamic light scattering (DLS),[12] in addition to the previously mentioned techniques.[7,9]

On the basis of evidence from these studies of the final films, the Toronto group hypothesized that under acidic conditions, mesoporous silica bodies (particles and thin films) grow through the continuous accretion of silicate micelles from solution onto surfactant−silicate "liquid-crystalline" seeds (∼50 nm in size).[12] For films grown at the air−water interface, it was speculated that these seeds organize into surface-confined, hexagonal domains oriented parallel to the surface through the influence of a surfactant hemi-micellar overstructure.[9,16,17]

Work at the Australian National University (Canberra group) suggests that this picture may not be complete.[22,28−30] Brown et al.[22,28] identified an induction period preceding the onset of mesoscopic order using in situ SANS and SAXS. While SANS measurements revealed that there was an accumulation of material at the interface during this time period, SAXS scans of the

(34) Manne, S.; Gaub, H. E. *Science* **1995**, *270*, 1480.
(35) Patrick, H. N.; Warr, G. G.; Manne, S.; Aksay, I. A. *Langmuir* **1999**, *15*, 1685.
(36) Helfrich, W. *Z. Naturforsch.* **1973**, *28C*, 693.

thin film early in the growth period did not detect mesoscopic order. Holt et al.[29] complemented this work with an in situ grazing incidence X-ray scattering (GIXS) study which showed that mesoscopic hexagonal order parallel to the interface appears by the end of the induction period. Ruggles et al.[30] reported GIXS evidence of an intermediate cubic phase structure and speculated that there may be structural evolution during the late stages of the induction period. The Canberra group interpreted these scattering studies as evidence of a transition from an amorphous phase to an ordered phase at the mesoscopic level. However, scattering data alone are unable to show how such a transition might occur. These results show that the growth of thin films is more complicated than originally envisioned by the Toronto group.

Here we are interested in attaining finer control over the structural organization of mesoscopic silica films. To this end, we consider the structural evolution of mesoscopic silica films grown under dilute, acidic conditions. We use electron microscopy to examine directly the mesoscopic and microscopic film structure at various times in the growth process. Direct observation of the film structure during growth provides the evidence necessary to explain the transition to order and clarifies the role of the interfacial interactions in determining structure. Our results confirm the view of the Canberra group that the film is initially disordered, demonstrate that ordered regions ("nuclei") appear within the disordered structure, and provide evidence that the ordered regions grow by inducing rearrangement of surrounding material. Our analysis shows that the final film consists of a polydomain mesoscopic structure. Moreover, we report evidence that the film is initially confined to the two-dimensional geometry of the air−water interface. Our work suggests that there is a characteristic film thickness at which energetic interactions with the interface are no longer sufficient to confine the film. We explain the structural evolution of the film during the transition to order at both the mesoscopic and microscopic length scales in terms of a disorder to order transition and interfacial interactions and discuss how mesostructural events influence the microscopic structure. Finally, we discuss the possibility of a universal growth mechanism for mesoscopic silica of all morphologies (e.g., films on solids, films at interfaces, and particles).

Experimental Section

Continuous mesoporous silica thin films were grown at the air−water interface. In our experiments, we used a dilute acidic aqueous system of tetraethoxysilane (TEOS, Fluka), the silicate source, and cetyltrimethylammonium chloride (CTAC, Aldrich), the cationic surfactant.[4] All reagents were used as received. Typical molar ratios ranged from 1 to 4 TEOS:1.2 CTAC:0.2−9.2 HCl:1000 H_2O. Previous work explored the highly acidic region ranging from pH −0.6 to 0.25.[9,16,18,26] Here we consider a milder range of acidic conditions (pH 0−2.0). The reagents were mixed, stirred vigorously for a minute to dissolve the TEOS, and left to stand for periods from a few hours to several weeks at room temperature. Each solution was divided into several aliquots. Since the films were continuous across the entire air−water interface, periodic collection of the films would subject later samples to disturbances introduced by the collection process. To prevent this, the aliquots were loaded in several identical containers, with films harvested from a given container only once. Some samples were sealed in airtight containers, while others were stored in covered Petri dishes. Films were also grown on freshly cleaved mica substrates under identical compositions for comparison.

Samples were collected onto TEM grids after elapsed times of 0, 4, and 9 h after loading into the storage container. For the 1 TEOS:1.1 CTAC:9.2 HCl:1000 H_2O system, these times were selected to allow sample collection during the induction period, the transition to order, and growth as an ordered film. Each sample was collected by dipping a gold TEM grid into the solution and lifting the film off the surface. Samples of the film were also collected several days to a week after mixing. These samples were air-dried, calcined (400 °C for 1 h) to remove the entrapped surfactant, embedded in resin (Epon Epoxy, Electron Microscopy Science), and ultramicrotomed (Leica Ultracut-UCT) for TEM analysis. These films were also examined by SEM. All investigations of film surface were performed on a Philips XL-30 Field-Emission SEM. The interior of the film was studied using cross-sectional TEM performed in a Philips CM 200 Field-Emission-Gun TEM (FEG-TEM) operated at 120 kV. TEM images and selected-area electron diffraction (SAED) patterns were acquired at both ambient and liquid nitrogen temperatures. A separate study confirmed that cooling the sample did not result in structural changes.[37] It is possible that the film samples collected in situ continued to evolve after collection (i.e., during the drying process). However, this is unlikely to introduce significant uncertainty as the sample drying time was only a few minutes. Additional concerns include distortions due to surface tension at the edge of the film and stresses due to evaporation. Images were taken at least 100 nm from the film edges to minimize complications due to these effects. Sample thicknesses were determined using standard electron energy loss spectroscopy (EELS) procedures.[38]

Results and Discussion

We present electron microscopy images for films grown in a solution of molar composition 1 TEOS:1.1 CTAC:9.2 HCl:1000 H_2O at room temperature under quiescent conditions. These conditions were chosen because they closely resemble previous work done by Aksay et al.,[18] and the UCSB,[4,21] Toronto,[9−12,16,17,20,24−26] and Canberra[22,28−30] groups. This offered a convenient basis for comparison. Under these conditions, a continuous film was observed visually after about 5 h. After 1 day, it was possible to extract wet films as large as the area of the container (100 cm^2). The solution turned cloudy after 8−10 h due to the formation of suspended particles. Most particles settled to the bottom of the container within a day. TEM samples were collected for electron microscopy analysis at regular intervals during film growth.

The films were initially smooth and developed wrinkles with time (usually after several days). The wrinkles varied in length (10−30 mm) and periodicity (∼1−10/cm), generally increasing in size with time. Sample collection disrupted the film surface, leaving a small hole where the grid penetrated the surface. Over time, the film regrew in these regions. Figure 1 shows a region where a sample was collected immediately upon transfer of the solution to the container. The picture was taken several days after sample collection. Immediately after sample collection, there was no evidence of any disruption. However, as the film grew thicker and developed

(37) We carefully compared SAED patterns obtained at both temperatures to verify that a temperature-induced phase change did not occur. No variations in crystal structure and symmetry were found.

(38) Leapman, R. D.; Fiori, C. E.; Swyt, C. R. *J. Microsc.* **1984**, *133*, 239.

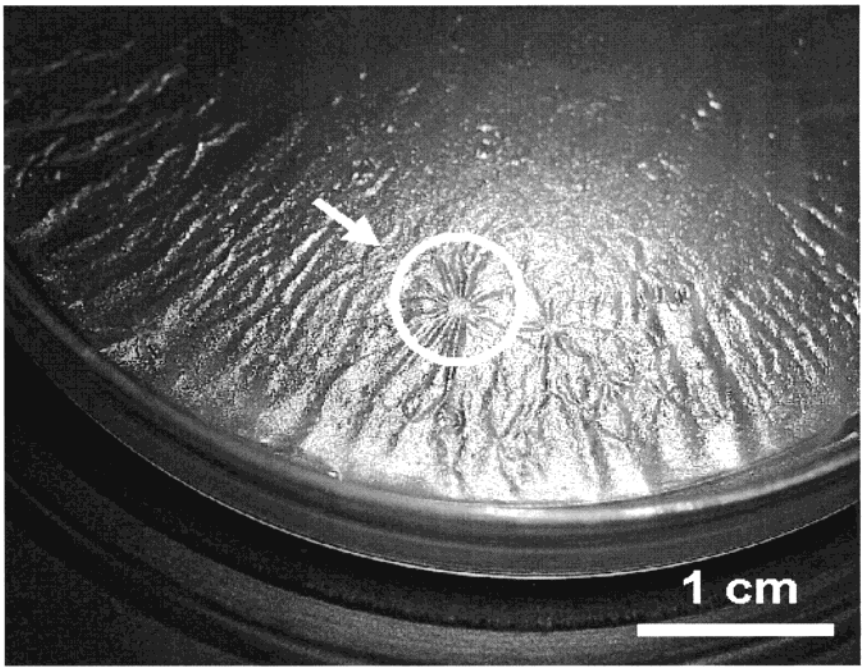

Figure 1. Region where a TEM sample was collected immediately upon transfer of the solution to the container ($t = 0$). The image represents conditions after 1 week of growth. The arrow indicates where the TEM grid was lifted through the surface. The wrinkling pattern suggests that structure appears at the air−water interface immediately after mixing. Molar composition: 1 TEOS:1.1 CTAC:9.2 HCl:1000 H_2O.

wrinkles, a defect pattern with the same size and shape as the TEM grid became visible. This suggests that some structure was present at the interface at the earliest stages of growth to record this perturbation. Under the conditions used, regrowth occurred through the first 2 days of growth. After 2 days, regrowth did not occur because the silica source was exhausted.[39]

Films were collected and dried as described in the Experimental Section. EELS showed that a sample collected after 5 h of growth had a thickness of ∼20 nm. Figure 2 shows TEM images of samples collected immediately after loading into the container and at 4 and 9 h of growth. The film contains a disordered structure. Our TEM studies did not uncover ordered mesoscopic structure in any film grown for less than 9 h under the growth conditions described. Both ordered and disordered regions were observed after 9 h. Figure 3 shows a typical cross-sectional TEM image of a film with regions of hexagonal order surrounded by regions where the channels are still disordered. This image was taken from a sample collected at the end of the induction period. The structure observed by TEM is consistent with X-ray scattering data reported by Brown et al.[22] and Holt et al.[29] Films collected after several days had mesoscopic order previously described in the literature (Figures 4 and 5). We also cross-sectioned the film parallel to the surface of the film (Figure 6). TEM analysis of the slices revealed the polycrystalline nature of the mesoscopic ordering.

Figure 4 is a representative cross-sectional TEM image of the film−water interface of a film grown for 2 days. We note that there appears to be a thin disordered region ∼20 nm thick at the film−water interface. Regular order is present in the film bulk with an average channel spacing of ∼4 nm. Typical cross-sectional TEM images perpendicular (Figure 5a) and parallel (Figure 5b) to the tubule direction confirm that the film contains channels lying roughly parallel to the interface. We also noted that the tubules were not always straight. For example, the side-view of the pores (Figure 5b) show them slanted relative to the horizontal edges. Additional insight into the mesoscopic evolution was gained by examining a thin section cut nearly parallel to the interface (Figure 6). The image in Figure 6 reveals two regions of distinct tubule orientation and a transition region between them. Careful examination of numerous samples sectioned in different orientations showed no gross defects such as dislocations or massive faults. The majority of the sections had regular packing. However, there are clearly regions where the material retains a disordered structure at the domain boundaries.

Nucleation and Growth: Disorder to Order Transition. Our results, coupled with already published data,[4,9,12,16,18,22−26,28−35] allow us to reconstruct the structural evolution of the film at both the mesoscopic and microscopic length scales. In this section, we outline our disorder to order transition model and briefly review analogous systems wherein a similar transformation occurs.

We agree with the Canberra group's view that the film grows through a multistep process. Our TEM analysis allows us to describe the process, in particular, the transition to order, in more detail. Our results indicate that silicate and surfactant moieties begin to accumulate at the air−water interface immediately upon mixing (Figures 1 and 2). The absence of Bragg peaks in the SAXS and SANS data imply that the film is initially amorphous.[22,28,29] AFM work of a dried film surface by Yang et al.[9] suggests that the transport of silicate and surfactant precursors to the interface occurs through the accretion of silica-coated micelles. It is

(39) We found that film regrowth could be initiated by adding additional TEOS to the system.

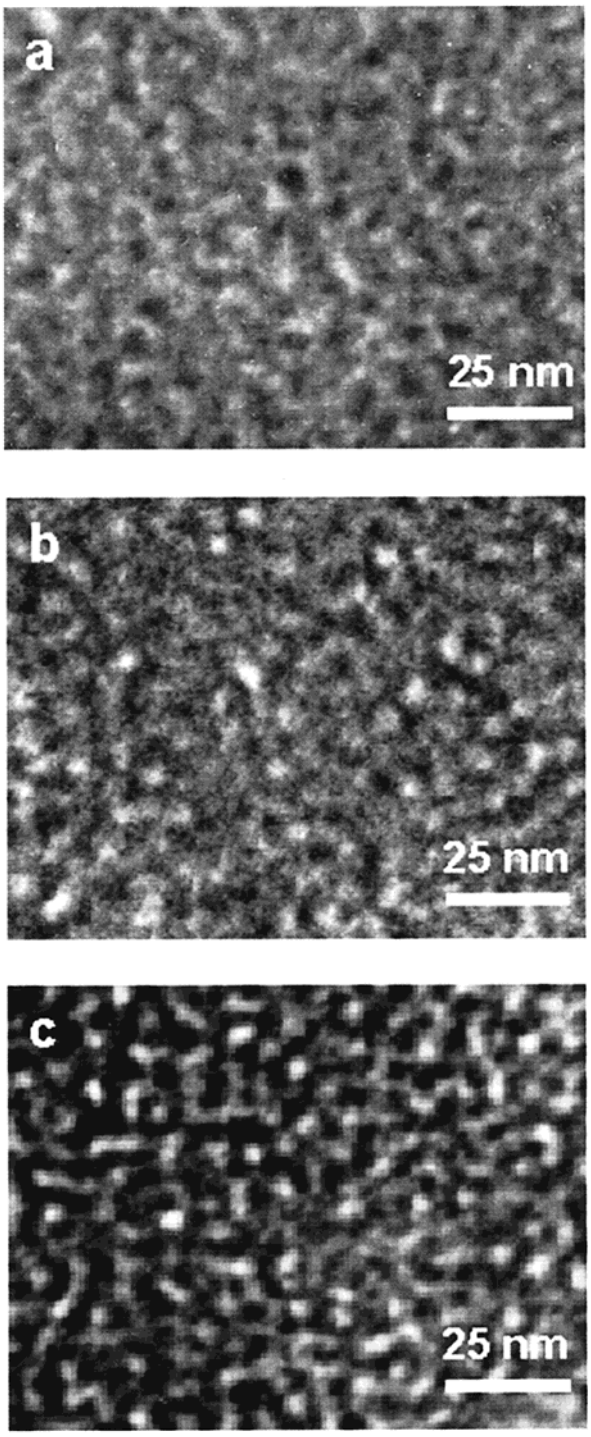

Figure 2. TEM images of samples collected on Au grids at elapsed times of 0 (a), 4 (b), and 9 h (c). These images indicate that disordered structure can be observed through the induction period.

believed that fresh silicate and surfactant is added to the film in this manner throughout film growth. Order arises in the film through the reorganization of a disordered phase in which the micellar channels form organized regions within the amorphous structure (Figure 3). The delay associated with the initial appearance of these ordered domains ("nuclei") corresponds roughly to the induction period observed by the Canberra group. Ordered domains promote the organization of surrounding material. In thin films, interfacial interactions impose an energetic constraint on the orientation of the channels. Consequently, the ordered regions are aligned parallel to the interface. The impingement of these domains leads to a film with the observed features.

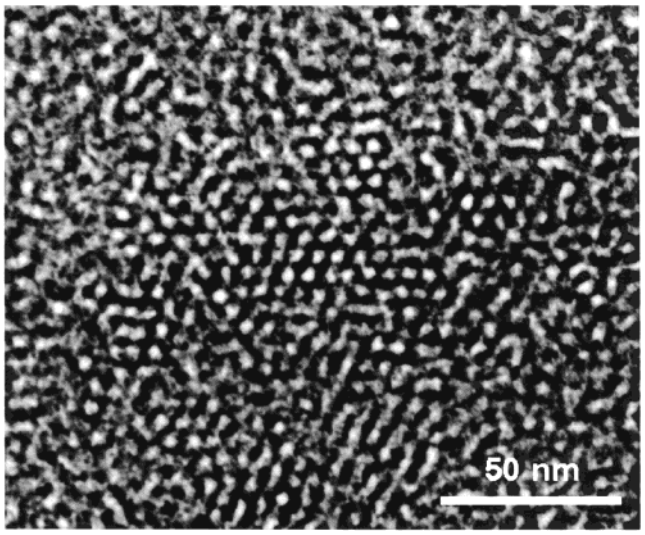

Figure 3. Cross-sectional TEM image of film collected at the end of the induction period. Regions with hexagonal close-packing order are surrounded by disordered material.

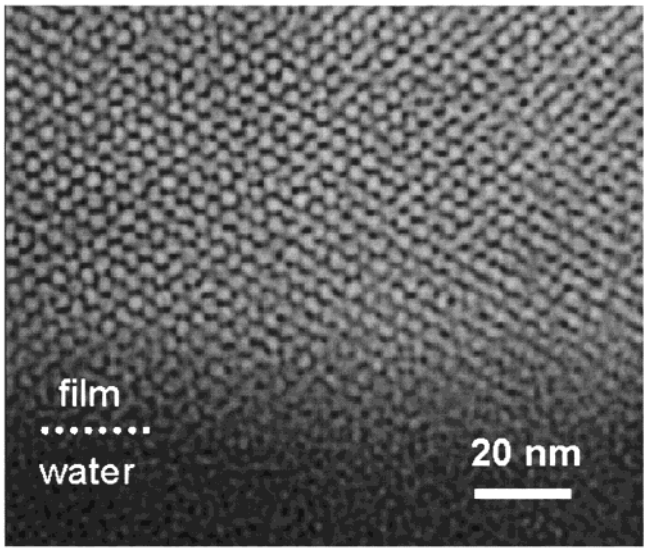

Figure 4. Cross-sectional TEM image of the final film near the water−film interface. The film was collected after 2 days of growth. The water−film interface is located at the top of the image.

A disorder to order transition is not an entirely new phenomenon. Lu et al. observed it for mesoscopic silica thin films formed by aerosol-based drying[15] and dip-coating.[23] They prepared mesoscopic silica nanoparticles by atomizing an ethanol-rich precursor solution. TEM analysis revealed that some of the resulting particles were ordered at the interfaces, but possessed disordered interiors.[15] Silica thin films using a dip-coating scheme in which the substrate was dipped vertically into an ethanol-rich solution. TEM analysis showed ordered regions at the substrate surface and at the air−water interface. The interior of the film was disordered.[23] Lu et al.[15,23] hypothesized that the evaporation of the solvent causes the local concentration at the air−water interface to increase, thereby triggering a transition to

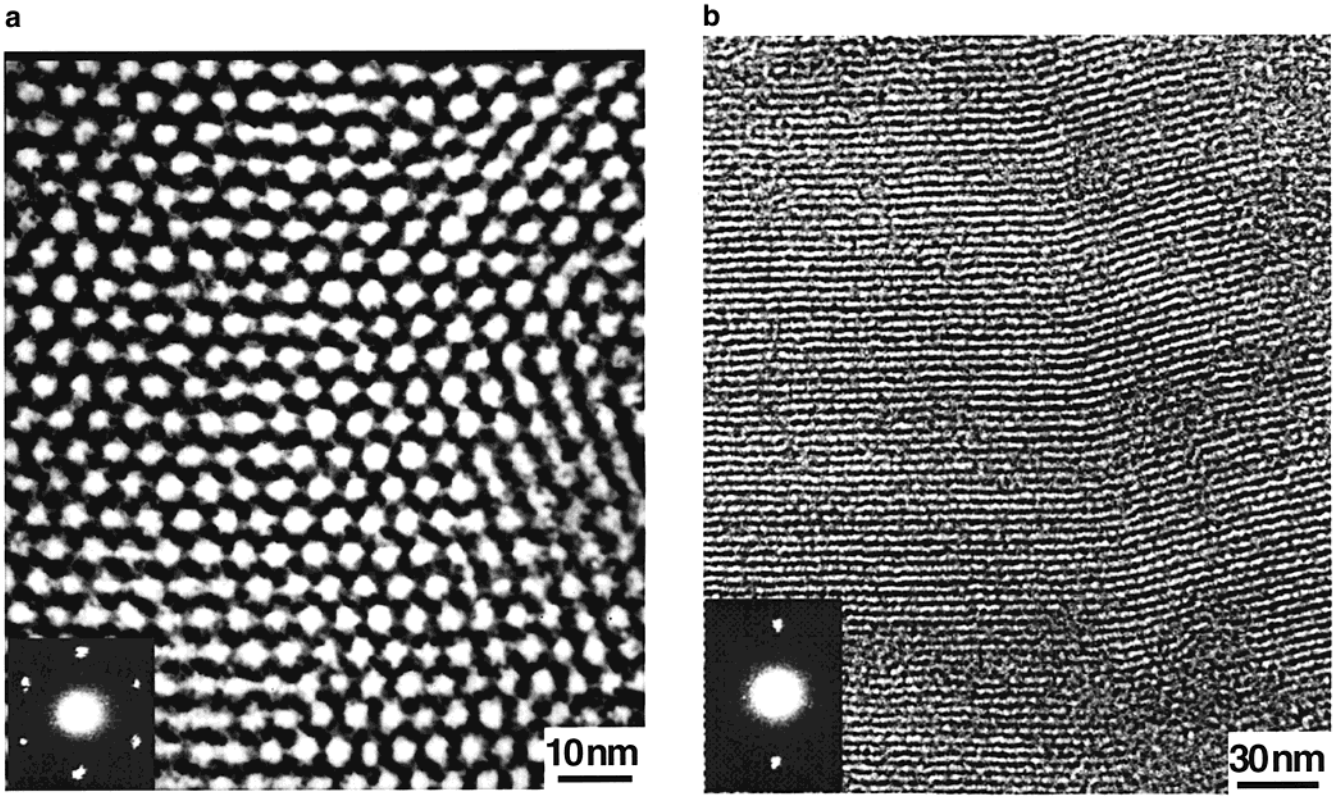

Figure 5. Cross-sectional TEM images of the final film interior, perpendicular to the film surface. Head-on (a) and side view (b) images are shown. Inset: SAED patterns indicating regular hexagonal packing and parallel channels. The channels in Figure 5a show a −5% to 10% strain in both the parallel and perpendicular directions. These values suggest that the film is not highly distorted. The Toronto group has suggested that drying stresses may be responsible.[14] We agree that drying is the most likely explanation for this observation. However, we note for *unconstrained* films (air−water) that the observed strain should be low. In situ GIXD analysis of the wet film did not reveal any deviations from a hexagonal lattice, supporting this claim.[29] This reasoning can be extended to films grown on solid substrates (constrained drying) and particles (unconstrained). Indeed, films grown on mica[24] possess a distorted bricklike structure near the interface while there is no mention in the literature of significant strain in the mesostructural order of particles. In Figure 5b, the 13° bend in the channel may be mesoscopic evidence of the 2D to 3D transition.

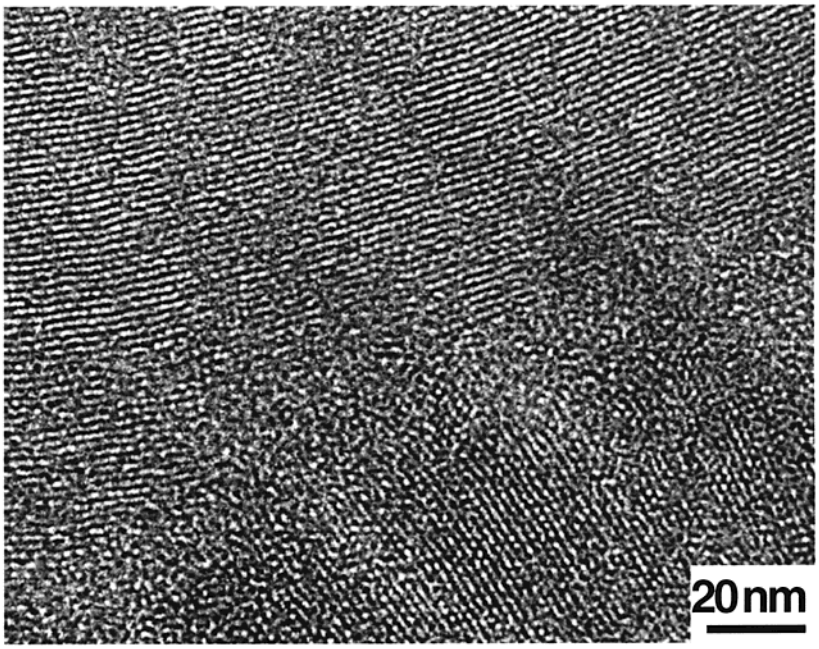

Figure 6. Cross-sectional TEM image of the final film interior, parallel to the film surface. Ordered domains can be clearly seen. Small pockets of disordered regions exist between the ordered domains.

order in the film. We note that although their films are formed on a much faster time scale and in the presence of a large excess of ethanol, their results are consistent with the generalized disorder to order transition mechanism described here. Moreover, Xu et al.[40] recently reported similar behavior during the biomimetic min-

eralization of calcium carbonate films. An amphiphilic porphyrin template was used to promote the growth of calcium carbonate films at an air−water interface. The calcium carbonate film consisted initially of a single amorphous phase which underwent a phase transformation into a polycrystalline structure. On the basis of these results, Xu et al.[40] concluded that the porphyrin-promoted nucleation and influenced the orientation of the structure through a solid-state nucleation and growth mechanism. Finally, the disorder to order transition has also been the subject of intense study in the block-copolymer melt community.[41]

Mesoscopic Structural Evolution: Alternate Channel Orientations. To date, studies of films grown at the air−water interface have typically revealed that the channels are hexagonally packed and oriented parallel to the interface.[13,14,22,26,28,29] This is also the case for films grown on solid substrates (e.g., mica and graphite).[9,18,24,25] This orientation and pore organization (Figure 5b), while strongly preferred, does not always occur. Figure 7 shows cross-sectional TEM images of regions where the channel organization differs markedly from the expected. A tilted channel orientation has been observed in some films (Figure 7a). We have also encountered regions where the channels are organized into a cubic arrangement (Figure 7b) rather than the more common hexagonal packing. SAXS confirmation of cubic channel organization was provided by Ruggles et al.[30] They further noted that over time, the cubic regions evolve into a hexagonal arrangement. Although previous work has shown it possible to attain a cubic phase arrangement by altering the composition of the precursor, the reasons behind coexisting cubic and hexagonal channel organization are still unclear.[3−5] These observations are consistent with the disorder to order transition model. Tilted nuclei, while energetically unfavorable, could easily give rise to the tubules seen in Figure 7a. Similarly, the spontaneous development of cubic rather that hexagonal order in some nuclei at the onset of the disorder to order transition could be responsible for the structure seen in Figure 7b. This also suggests the possibility of order to order transitions.

Microscopic Structural Evolution: Ribbons and Voids. The structural features and evolution of the film at a microscopic scale was studied using SEM. Images of the air−film and film−water interface (Figure 8) and cross-section (Figure 9) provide additional evidence of a stepwise growth mechanism. Images of the air−film and water−film interfaces for films grown for 2 days are shown in Figure 8. They possess ribbonlike features similar to those reported for particles and thin films grown on mica, graphite, and silica.[9,18,24,25] These ribbons generally meander in two dimensions (parallel to the interface). The low magnification image in Figure 8a shows the difference between the air and water sides of the film. The air side of the film (Figure 8b) appears to be comprised of smooth ribbons, which lie in the plane of the film. There appears to be no underlying directionality in domain orientation. By comparison, the structural features of films grown on mica and graphite

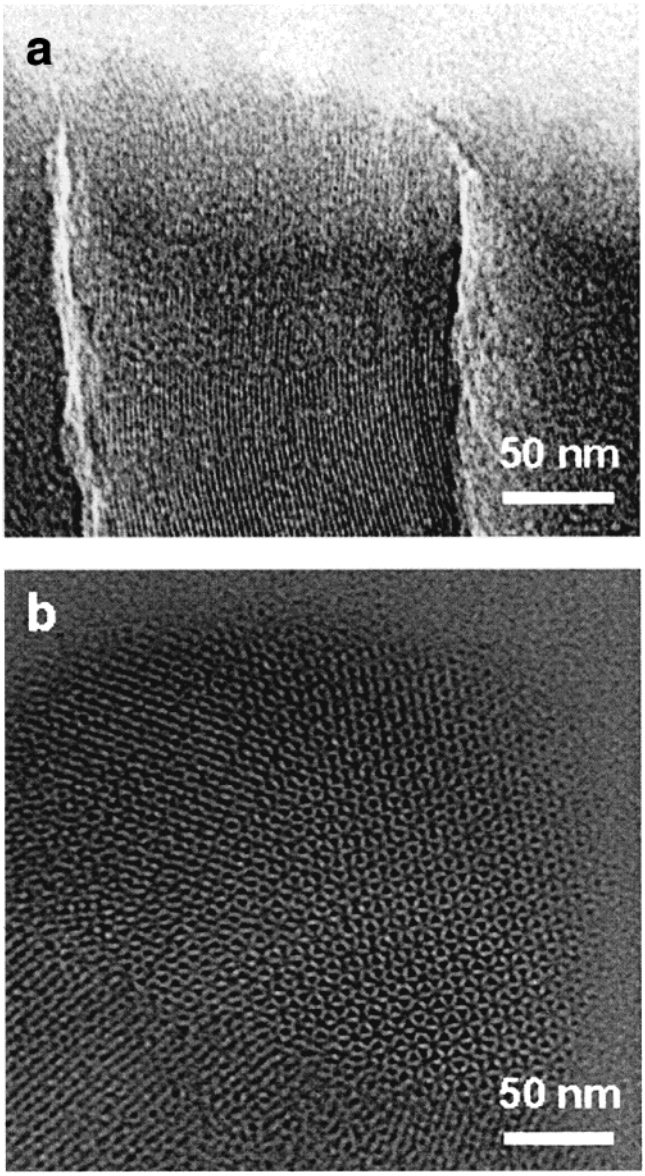

Figure 7. Cross-sectional TEM image at the film−water interface of films grown for 2 days showing additional channel orientations. Channels are sometimes inclined relative to the surface (a) and ordered in a cubic phase (b). The large, vertical stripelike features in image (a) are wrinkles in the film cross-section.

exhibit preferred orientations at both mesoscopic and microscopic length scales.[18] Similarly, more pronounced ribbons are visible on the water side of the film (Figure 8c). There are also regions where the ribbon protrudes out of the plane of the surface. Microindentations and triangular pits can be seen on both sides of the film. Significant variation in the size and shape of these pits was seen across the surface of the film. The water side of the film reveals cracks and rougher texture.

The texture and microindentations may be the microscopic manifestations of the rearrangement of the amorphous material into packed channels. It has been suggested that these pits result from the impingement of physically distinct domains of material as they grow in size through accretion.[17] Although this mechanism maybe operative at the water−film interface, it does not account for the presence of microindentations on the air−film side. Our disorder to order transition model

(40) Xu, G.; Yao, N.; Aksay, I. A.; Groves, J. T. *J. Am. Chem. Soc.* **1998**, *120*, 11977.
(41) Newstein, M. C.; Garetz, B. A.; Balsara, N. P.; Chang, M. Y.; Dai, H. J. *Macromolecules* **1998** *31*, 64.

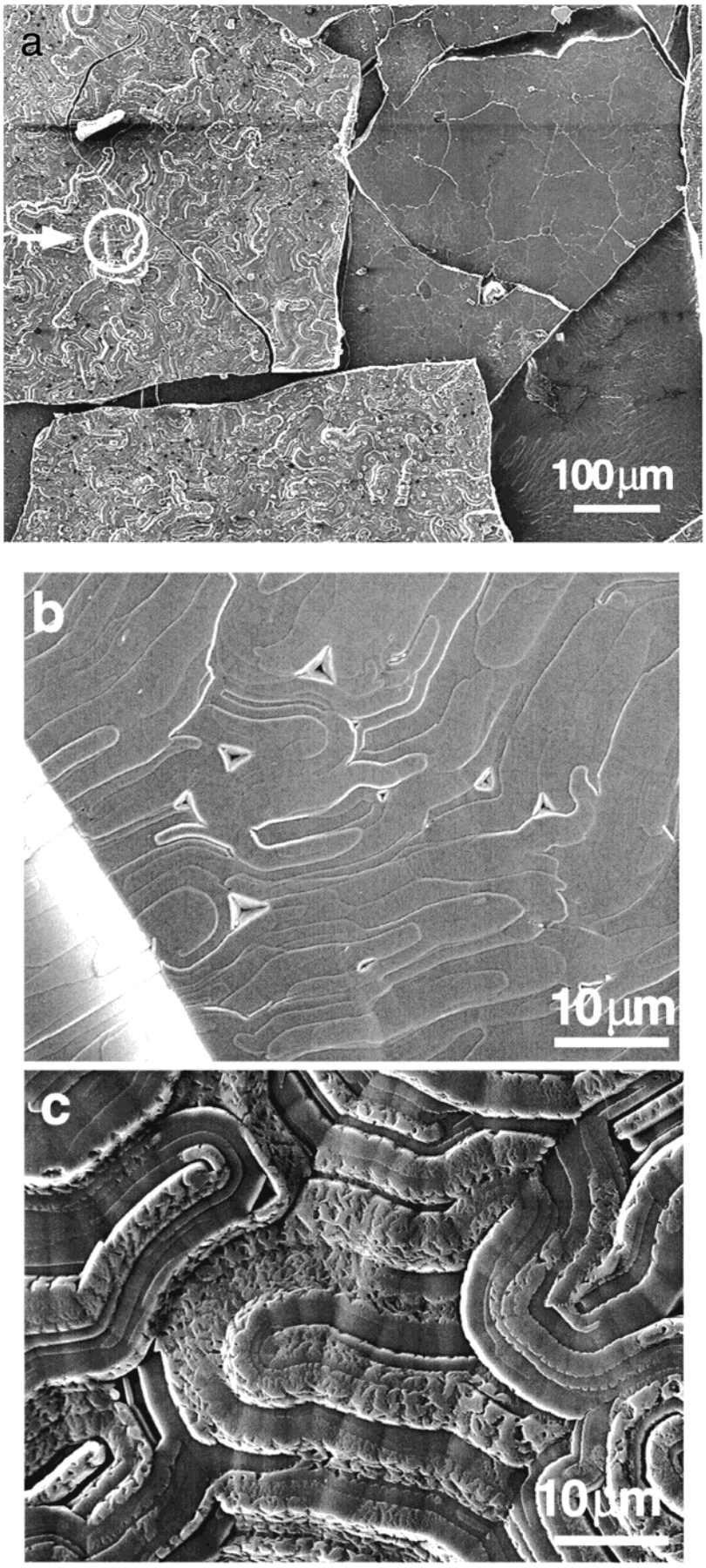

Figure 8. SEM images of the film grown at the air−water interface. Low magnification reveals different microscopic features are observed on the air (right) and water (left) sides (a). The fine cracks on the air side are mechanical in nature and due to sample preparation. Close-up view of the air−film (b) and film−water (c) surfaces are shown.

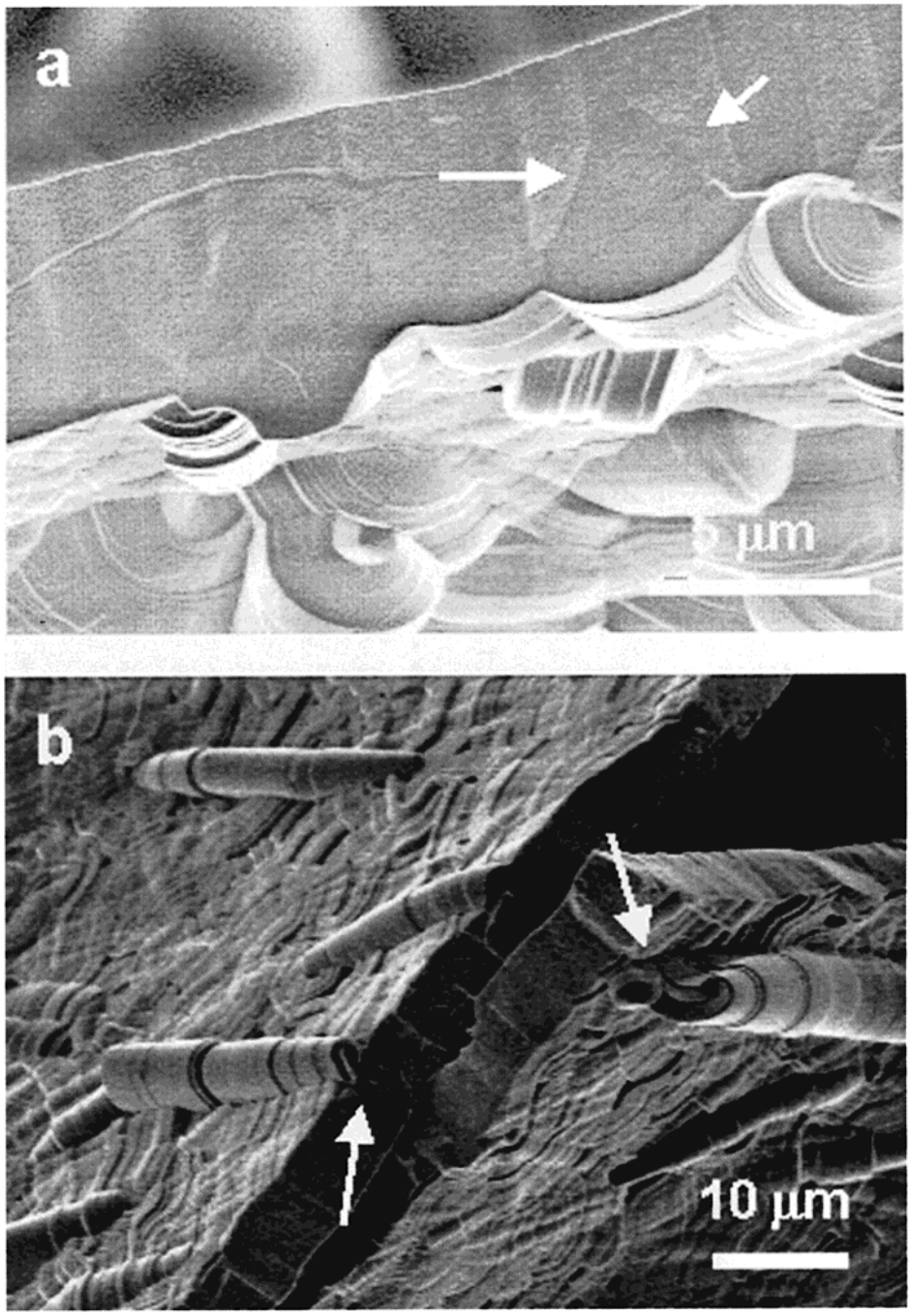

Figure 9. Typical cross-sectional SEM images of films viewed nearly parallel to the surface reveals that the particle-like ribbons are a continuous part of the film and shows more pronounced ribbon protrusions. Images are taken from films grown at pH = 0.5 (a) and pH = 0 (b).

offers a different explanation for these microscopic features. We note that the mesoscopic silica densifies during the growth process. This occurs through two pathways—the rearrangement of the disordered material into well-packed channels and continued silica polymerization.[42] Densification of the amorphous phase around multiple nucleation sites throughout the amorphous phase (whether induced by silica polymerization or the disorder to order transition) explains the formation of voids within the body. This phenomenon has been encountered in the glass−ceramics community under the guise of void and crack formation during aging.[43,44]

Interfacial Interactions: Transition from In-Plane (2D) to Unconstrained (3D) Growth. Near the interface, both the ribbons and mesoscopic channels (usually) are oriented parallel to the surface. As discussed previously, in-plane confinement may be due to Helfrich-type interaction and/or an interface−micelle energetic interaction. The energetic interaction imposed by the interface diminishes as the film grows thicker; at some critical length, the ribbon is no longer confined

(42) Brinker, C. J.; Scherer, G. W. *Sol−Gel Science*; Academic Press, Inc.: New York, 1990.

(43) Kingery, W. D.; Bowen, H. K.; Uhlmann, D. R. *Introduction to Ceramics*; John Wiley and Sons, Inc.: New York, 1976.

(44) Beall, G. H. *Properties and Process Development in Glass-Ceramic Materials; in Glass: Current Issues*; Wright, A. F., Dupuy, J., Eds.; NATO ASI Series, Series E: Applied Sciences- No. 92; M. Nijhoff, 1985; pp 21−48.

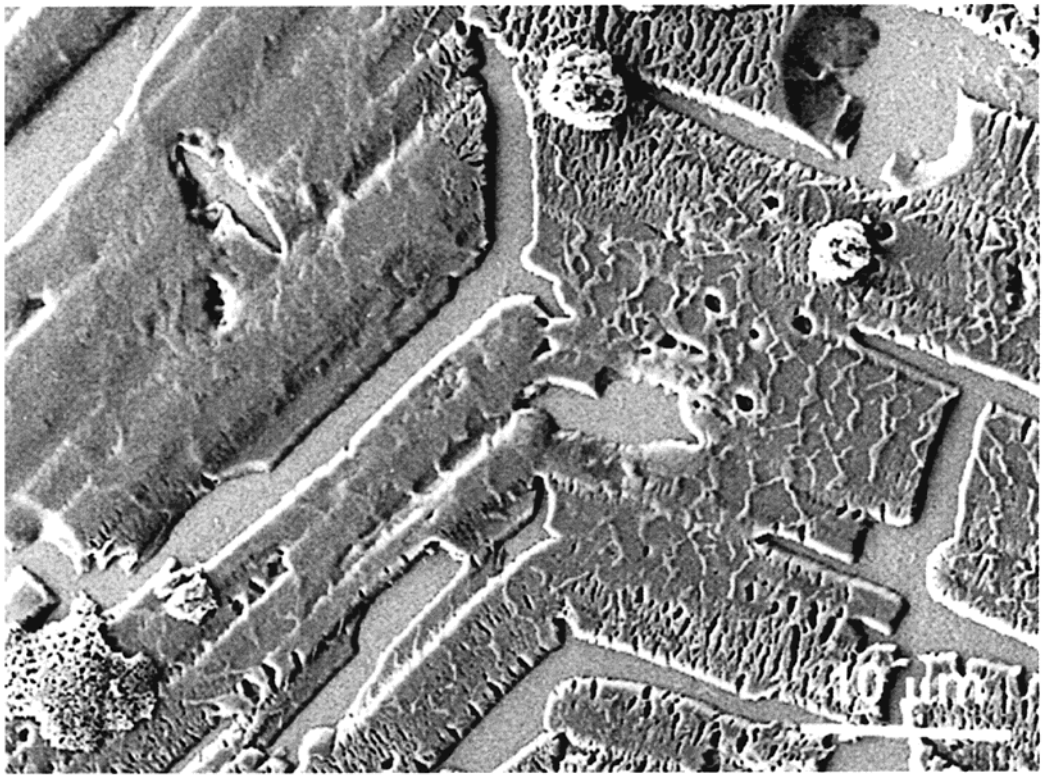

Figure 10. SEM image of film grown on a mica surface for 2 days.

and begins to curl in three dimensions. The critical thickness is expected to be larger for strongly interacting surfaces, such as graphite and mica, and smaller for more weakly interacting surfaces, such as silica and the air−water interface, supporting our model. This framework predicts particle formation in the limit of no interfacial interactions.

Examination of film cross sections showed that the protruding ribbons are a natural consequence of growth. Typical cross sections are shown in Figure 9. The figures show that the ribbon protrusion begins part way through the film. The pH of the growth solution appears to influence the extent of the protrusion. This can be seen by comparing the features grown at pH = 0.5 (Figure 9a) with those of films grown at pH = 0 (Figure 9b). We noted that as pH dropped, the protrusions on the films were generally longer. We examined numerous samples and did not find any films where the ribbon protrusions began immediately at the air−film interface. There appeared to be a thickness threshold (∼1−2 μm) below which protrusions were not observed.

We further explored the idea of a critical thickness for the transition to three-dimensional growth and the role of the interface by examining two limiting cases. We grew thin films on mica to investigate the possibility of a critical thickness for films grown on solid, strongly interacting substrates. We also considered the limit of no interfacial effect by collecting particles from solution. The films grown on mica substrates up to a few micrometers in thickness (Figure 10) possess ribbons that remain in the plane and are oriented in two directions consistent with our previous work.[18] They did not appear to have any significant ribbon protrusions, which suggests that there the critical thickness for films grown on solid, strongly interacting substrates was not exceeded. Thicker films (grown for longer periods) did possess ribbon protrusions. Our model is further supported by the presence of ribbon protrusions from films several microns thick grown on silica substrates.[18]

The microscopic curvature observed in film ribbons (and particles) has been explained previously using a liquid-crystal defect model proposed by Feng et al.[31] for alkaline systems and Yang et al.[26] for acidic systems. The liquid-crystal defect model is both compatible and complementary to our disorder to order transition model. The presence of defects in the initial ordered regions could be amplified into large curved domains under our proposed growth mechanism. Interfacial interactions near an interface may suppress this effect for very thin films. However, once the film thickness surpasses a characteristic value, liquid-crystal defects could readily lead to the three-dimensional features observed in the ribbon protrusions.

Finally, strongly interacting surfaces such as graphite and mica bias the orientations of the initial domains resulting in alignment at length scales on the order of hundreds of nanometers and higher (in-plane orientation). Once formed, these crystalline regions can direct the ordering of disordered material that has freshly accumulated at the film−water interface. In this way, the mesoscopic ordering parallel to the interface is propagated through the film.

Mechanistic Parallels to Particle Growth. We considered the possibility that the structural evolution of particles parallels that of films, by collecting particles from solution at various times. Particles collected from solution immediately upon clouding and after several days of growth are shown in Figure 11. Particles grown for several days contain ribbons (Figure 11a) and microindentations (Figure 11b). Since the growth of particles in solution represents the limit where the

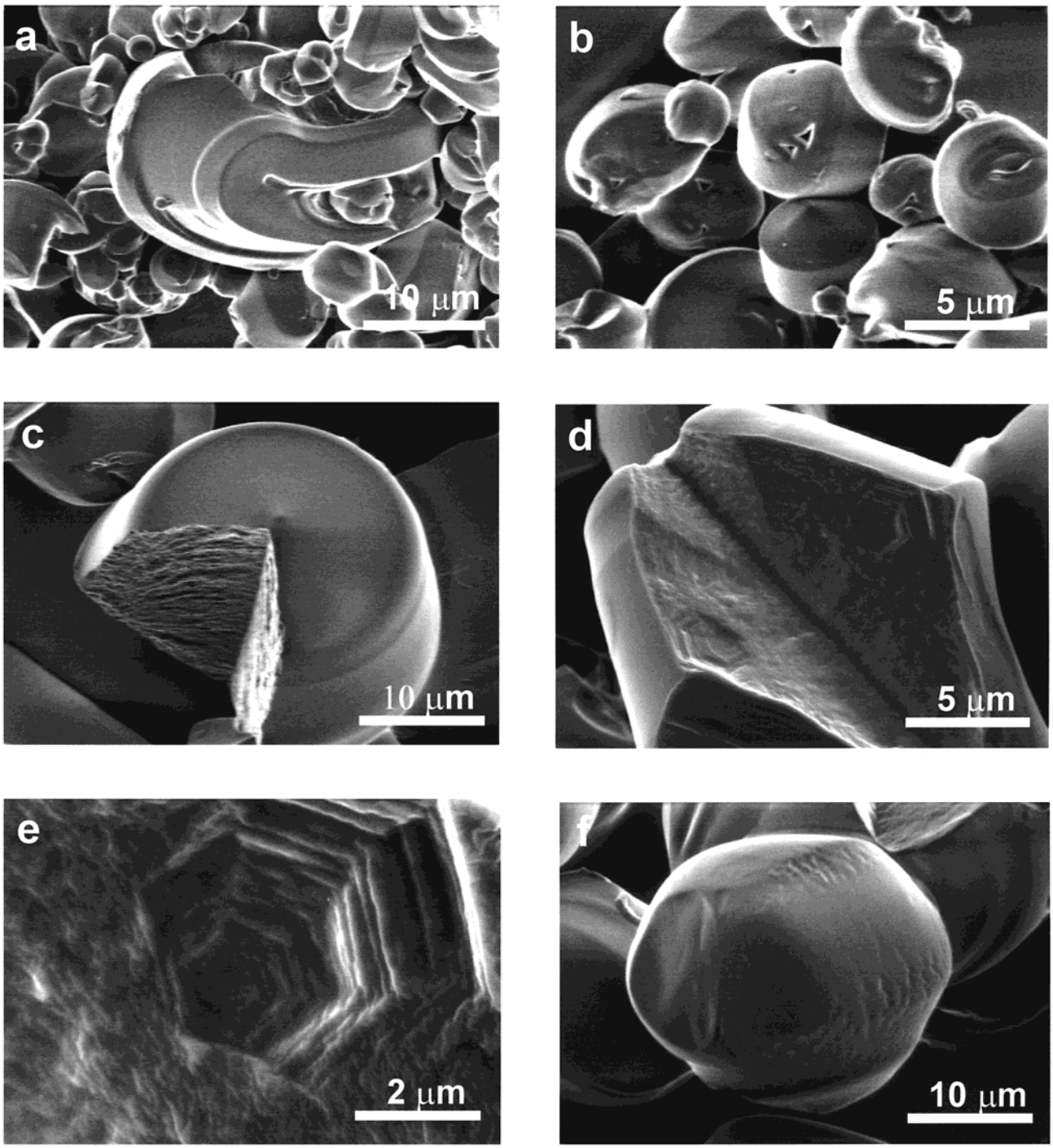

Figure 11. Particles were collected immediately upon clouding of the solution by filtering the sample (a, b) and from the bottom of the container after several days of growth (c−f). SEM images of particles collected after several days of growth show (a) projected ribbons and (b) microindentations. Drying caused many of the particles to break open, exposing internal structure (c). The hexagonal structure near the equator may be evidence of an analogous disorder to order transition in particles (d and e). Some particles collected upon clouding lacked the well-defined gyroidal structure found after extended growth (f).

meandering of the ribbons is not constrained to two dimensions, the presence of ribbon-protrusion features supports the idea of a common mechanism for growth. Furthermore, microindentations suggest that a disorder to order transition may be occurring. Particles were collected immediately upon clouding of the solution to test this hypothesis. Many particles cracked upon drying, revealing a disordered internal structure (Figure 11c). In some cases, ordered structures were observed (Figure 11d). The hexagonal shape of the structure (Figure 11e) and the fact that it is embedded within the particle suggest mesoscopically ordered domains may be present in particles as well as films. Finally, some of the particles collected upon clouding of the solution resembled the gyroids observed after longer periods of growth, but lacked well-defined edges (Figure 11f). This, too, is consistent with the notion that particles may initially be disordered. The disorder to order transition may be responsible for the development of well-defined edges in gyroid particles.

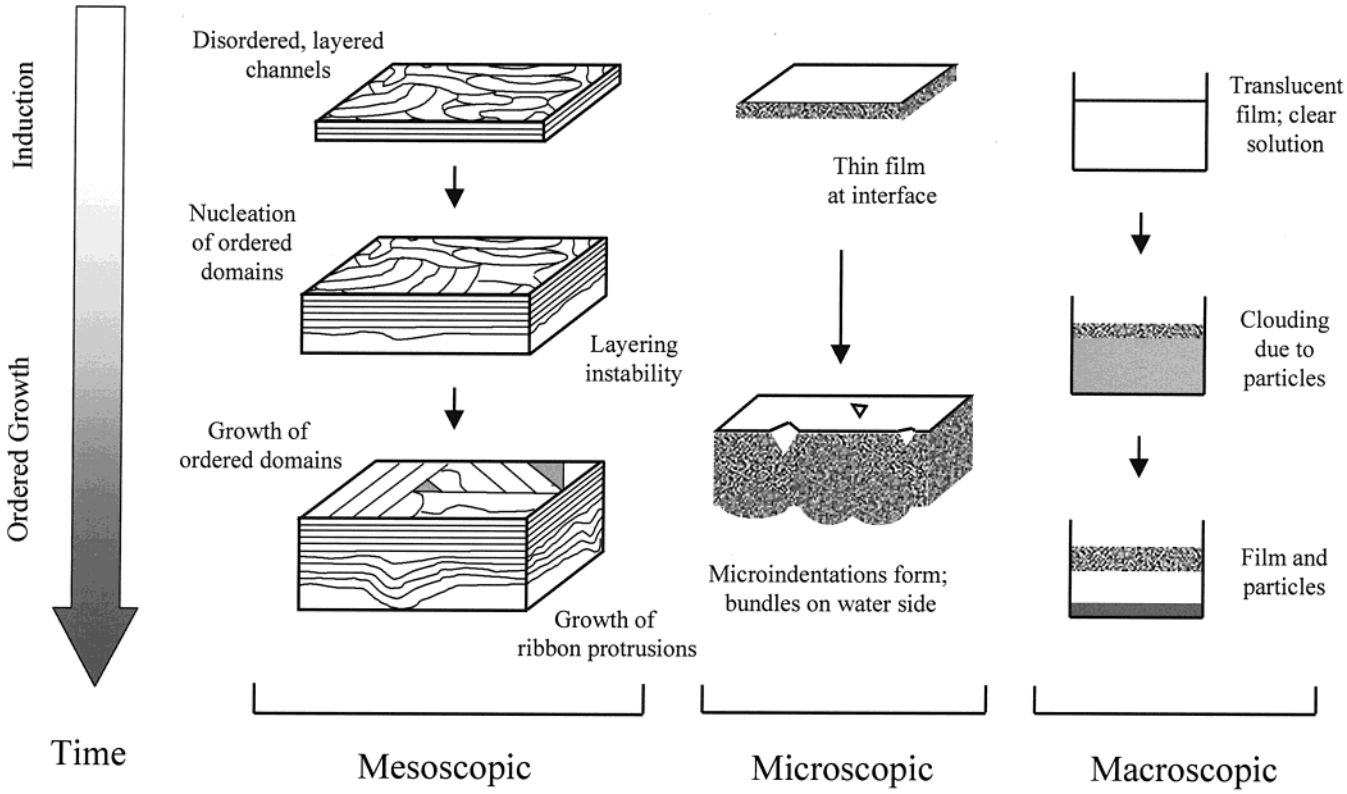

Figure 12. Schematic of proposed solid-state crystallization mechanism. Events are described at three length scales: mesoscopic (nanometer), microscopic (micrometer), and macroscopic (millimeter).

The intermediate structure seen in Figure 11f might be explained by the existence of multiple *amorphous* domains. Support for this notion comes from a study of the gyroid to sphere transition by Yang et al.[11] They found that this transition was caused by decreasing the acidity of the precursor solution. Interestingly, they found that spheres were less well-ordered (wider XRD peaks). They also include a catalog of particle intermediates between sphere and gyroid. Several of the structures appear to consist of individual domains. Although our observed gyroid-sphere intermediates result from a time rather than solution chemistry difference, we speculate that domains may be present at the earliest stages of particle formation (possibly preceding the onset of mesoscopic order).

Given the structural evolution observed in films and our observations of particles collected immediately upon clouding, we suspect that the current model of particle growth from liquid-crystalline seeds[12] may also be incomplete. A common mechanism in which particles begin as disordered silicate−surfactant assemblies which mesoscopically crystallize after some induction period, may be operative.

Implications. Our observation that the film exhibits a disordered to ordered transition in the solid phase leads to several interesting implications. First, it confirms that order arises in the film through a multistep process rather than through a direct growth of multiple mesoscopic crystals from solution. Second, it suggests that conditions early in the process (especially those which can influence the nucleation of ordered domains) can have a marked effect on the final film structure by influencing the size and alignment of the initial ordered domains. This, in turn, points to the possibility of tailoring the film structure through the application of an external field. Indeed, Trau et al.,[19] Tolbert et al.,[45] and Hillhouse et al.[46] reported the successful orientation of mesoscopic materials using electric, magnetic and shear fields, respectively. Finally, it presents a starting point for developing an unified mechanism for the growth of mesoporous silica of all morphologies. Work by Firouzi et al.[32] has demonstrated that, under alkaline conditions, phase transitions can occur within the liquid crystalline surfactant−silicate mesophase. Regev observed liquid-crystalline seeds using cryo-TEM.[33] These observations suggest that the disorder to order transition in the condensed phase may be a general phenomenon in the development of order in mesoscopic silica.

A number of exciting engineering ramifications arise from the fact that the film develops ordered structure over time. If the film is pliable at early stages, processing conditions may be adjusted to produce films of a specified thickness, homogeneity, pore alignment, and orientation.

Conclusions

The structural evolution of mesoscopic silica thin films grown at the air−water interface was monitored using electron microscopy. The films are initially amorphous in nature and remain so during an induction period. Direct observation has allowed us to detail the mecha-

(45) Tolbert, S. H.; Firouzi, A.; Stucky, G. D.; Chmelka, B. F. *Science* **1997**, *278*, 264.
(46) Hillhouse, H. W.; van Egmond, J. W.; Tsapatsis, M. *Langmuir* **1999**, *15*, 4544.

nism for the transition to order in mesoscopic thin films grown at air−water interfaces. We have shown that after the induction period, the films develop mesoscopic order by the nucleation of ordered regions, which are influenced by the presence of an interface. Once order is established, the films develop regular packing through the ordering of disordered regions within the film. The film grows in thickness through the accretion of material from the precursor solution. Deposited material initially forms disordered channels, but relaxes to the ordered state under the influence of the ordered domains. Mass constraints imposed by densification through silica polymerization and the disorder to order transition account for some of the microscopic topological features. The transition from two-dimensional growth (in-plane confinement) to three-dimensional growth (unconstrained growth) appears to occur at some critical length. This is evidenced in the microscopic structure of the film.

Acknowledgment. This work was supported by the U.S. Army Research Office (grant DAAH04-95-0102 and the National Science Foundation MRSEC program (grant DMR98-09483) Discussions with Dan Dabbs and Linbo Zhou are appreciated.

CM000038A